NISTIR 6030

THIRTEENTH MEETING OF THE UJNR PANEL ON FIRE RESEARCH AND SAFETY, MARCH 13-20, 1996

VOLUME 1

Kellie Ann Beall, Editor

June 1997
Building and Fire Research Laboratory
National Institute of Standards and Technology
Gaithersburg, MD 20899

U.S. Department of Commerce
William M. Daley, *Secretary*
Technology Administration
Gary R. Bachula, *Acting Under Secretary for Technology*
National Institute of Standards and Technology
Robert E. Hebner, *Acting Director*

Measurements and Predictions of the Velocity Field Induced by Pool Fires

X. C. Zhou and J. P. Gore
Thermal Sciences and Propulsion Center
School of Mechanical Engineering
Purdue University
West Lafayette, IN 47907

Howard R. Baum
Center for Fire Research, Building and Fire Research Laboratory
National Institute of Standards and Technology
Gaithersburg, MD 20899

Introduction

Due to the importance of the air entrainment rate in determining fire size, radiation properties, and soot production, various techniques have been applied to its measurement. The measurement techniques can be roughly classified into four categories. The first category involves monitoring of the air flow rate needed to meet the entrainment requirement of the fire while maintaining ambient pressure [1, 2]. The second category is to sample combustion products and solve a set of global mass balance equations to obtain equivalence ratio and hence the entrainment rate [3-5]. The third category involves measurement of the velocity and the temperature profiles inside the flame and subsequent calculation of the axial flow rate by either direct radial integration or integration of resulting curve fits [6-8]. One common disadvantage of the above three experimental methods is that information about the details of the entrainment flow field itself is not obtained. The fourth measurement category addresses the problem by obtaining detailed measurements of the flow induced by the fire [9, 10]. In Ref.[10], the mean and the fluctuating velocity field around a 7.1 cm toluene pool fire was mapped with a Laser Doppler Velocimeter (LDV). It was found that the value of the entrainment rate depends strongly on its definition implied by the first three measurement categories. In addition to the experimental work, a few studies involving analyses and computations of the entrainment flow field have also been reported [11, 12]. Taylor [11] calculated the air flow outside a thermal jet originating from a point source with the assumption that the entrainment rate is proportional to the jet velocity. Utilizing published experimental data, Baum and McCaffrey [12] applied a kinematic approach to predict the flow pattern induced by unconfined fires. The present paper reports application and extension of their methodology to the prediction of the entrainment flow field around 7.1 cm and 15 cm pool fires burning heptane and toluene.

The flow field is first decomposed into an irrotational flow and an incompressible flow component. The nonhomogeneous source terms in the partial differential equations governing these two flows, namely the volumetric heat release rate distribution and the vorticity distribution, are calculated from correlations given by McCaffrey [13]. The boundary conditions for the irrotational flow equation are approximated by an asymptotic solution to the potential flow generated by a point heat source, while the boundary conditions for the solenoidal flow are obtained by transforming the original equation into spherical coordinates and solving the resulting ordinary differential equation. In the present work, the analysis was extended to the case of a pool fire without a floor. The results show that the presence of a floor around the fire changes the entrainment flow field dramatically. Comparison of the predictions with velocity data obtained in the laboratory using a Particle Imaging Velocimetry (PIV) system are made and possible reasons for the discrepancies are discussed.

Theoretical Analysis

The entrainment flow velocity $\vec{V}^*$ is first decomposed into two components, namely the irrotational velocity $\overline{V}^*$ and the incompressible velocity $\tilde{V}^*$. The irrotational velocity field and the incompressible velocity field can be expressed in terms of a potential function ϕ^* and a stream function ψ^* as:

$$\overline{V}^* = \frac{\partial \phi^*}{\partial z^*}\hat{e}_z + \frac{\partial \phi^*}{\partial r^*}\hat{e}_r \qquad \tilde{V}^* = \frac{1}{r^*}\frac{\partial \psi^*}{\partial r^*}\hat{e}_z - \frac{1}{r^*}\frac{\partial \psi^*}{\partial z^*}\hat{e}_r \tag{1}$$

where the superscript * indicates a dimensional quantity. Following the nondimensionalization of Ref. [12] and representing the resulting nondimensional quantities with identical symbol without the asterisk, the governing equations in a nondimensional axisymmetric cylindrical coordinate system can be written as

$$\frac{\partial^2 \phi}{\partial z^2} + \frac{1}{r}\frac{\partial}{\partial r}\left(r\frac{\partial \phi}{\partial r}\right) = Q(\vec{r}) \tag{2}$$

$$\frac{\partial^2 \psi}{\partial z^2} + \frac{\partial^2 \psi}{\partial r^2} - \frac{1}{r}\frac{\partial \psi}{\partial r} = r\omega_\theta(\vec{r}) \tag{3}$$

As in Ref. [12], the nondimensional source terms in the two equations, $Q(\vec{r})$ and $\omega_\theta(\vec{r})$, are estimated using the correlations of buoyant diffusion flame structure given by McCaffrey [13]. Gaussian distributions are assumed for radial profiles of both velocity and excess temperature. Flame radius at different heights is calculated in closed analytical form following the procedure of Ref. [12]. The boundary conditions along the floor (as in [12]) are:

$$\frac{\partial \phi}{\partial z} = 0, \quad \psi = 0 \quad \text{at } z=0 \text{ for all } r \tag{4}$$

$$\frac{\partial \phi}{\partial r} = 0, \quad \psi = 0 \quad \text{at } r=0 \text{ for all } z \tag{5}$$

The boundary conditions for the velocity potential at the outer edge of computational domain are taken to be equal to those of a potential flow caused by an equivalent normalized point heat source $(1-\eta)$, where η is the radiative loss fraction:

$$\phi = \frac{1-\eta}{2\pi\sqrt{r^2+z^2}} \tag{6}$$

The boundary values of the stream function are obtained by transforming the elliptical partial differential eq. (3) into an ordinary differential equation in the spherical coordinate system. Substituting $\psi = \rho^{5/3}F(\mu)$, where $\rho = \sqrt{r^2+z^2}$, $\mu = \cos\theta$, and θ is the polar angle, into eq. (3) yields:

$$\frac{d^2F}{d\mu^2} + \frac{10F}{9(1-\mu^2)} = \Omega(\mu) \tag{7}$$

where $\Omega(\mu)$ is the normalized vorticity in the far filed. At the floor, μ is equal to zero and along the centerline, μ is equal to unity, while the stream function is zero at both locations, thus the boundary conditions for eq. (7) are:

$$F(0) = F(1) = 0 \tag{8}$$

Equation (7) with boundary conditions (8) is solved numerically to obtain a value of $F(\mu)$.

For the case of a buoyant fire without a floor, at the centerline eq. (6) still holds. However, along the outer edge, the velocity potential is half of that given by eq. (6). The F for a fire without a floor is calculated by solving eq. (7) with the boundary conditions:

$$F(-1) = F(1) = 0 \tag{9}$$

Equations (2) and (3) are solved using a finite difference method subject to the boundary conditions discussed above and the volumetric heat release rate field and the distribution of the azimuthal vorticity field given in [12]. The stream function yields the solenoidal velocity field $\tilde{V}$, which is induced by the vorticity generated by the buoyancy in the flame, and the velocity potential yields $\overline{V}$, the irrotational expansion of hot gases in the flame. The entrainment velocity field is the sum of these two components.

Experimental Methods

A fire burning heptane or toluene is stablized on a 15 cm pool in a 1.5m×1.5m×4m enclosure. The top 1 m of the enclosure is made of glass in order to establish an upper layer as the downstream boundary condition for the fire. The remaining 3 m of the enclosure is constructed using a fine wire cloth to protect the fire from ambient disturbances. The lip height (the distance from the fuel surface to the burner edge) is 0.8 cm in the case with no floor. With a 51cm sheet metal floor placed around the pool, the lip height had to be increased to 1.5 cm to avoid the establishment of flames at much larger radius on the floor. The burning rate dropped from 385 mg/s to 360 mg/s with the increased lip height, probably due to the decrease in the area of heat transfer to the fuel. The enclosure is seeded with Al_2O_3 particles of 0.5 μm mean diameter using a bank of specially developed seeders.

The configuration of the PIV system (FFD Inc.) is shown schematically in Fig. 1. A CW Argon-ion laser with a multiline power of 12 W is used to generate a train of dual pulses by passing through a two-slot chopper plate rotating at a frequency of 100 Hz. A cylindrical lens is used to illuminte a section of the flow field for two closely spaced short time intervals. A 1.4 MB CCD camera and a frame grabber are used to capture the light scattered from the seeding particles in the view region during the two laser pulses. To eliminate the ambiguity in the direction of motion, a shift in the direction of the mean velocity is introduced by a scanning mirror, which is synchronized to the chopper with a digital delay. The shift is larger in magnitude than the maximum reverse flow velocity to ensure a correct ordering of the two exposures. The images are processed with a resolution box of the size 32 × 32 pixels (corresponding to 2.5 × 2.5 mm in the flow field). The shift is subtracted from the resolved vector field in the analysis stage. The mean velocity field is obtained by averaging 100 instantaneous vector plots.

Results and Discussion

Predictions of the velocity field around the pool fire have been obtained using the model discussed above. Figure 2 shows the predicted entrainment flow pattern around a 15 cm heptane pool fire at a heat release rate of 17.4 KW and η=0.3. Near the floor, the flow is almost horizontal and without significant change in magnitude with radial distance. This is the mechanism by which a fire can cause strong inward wind. Near the fire, the velocity turns upwards, due to an intense source of vorticity caused by the density gradient. The magnitude of the velocity increases significantly in the near flame region, due to a combination of reduced flow area and an increase in the temperature. At greater distances from the floor, the flow is predominantly vertical. Figure 3 depicts the entrainment flow induced by the same fire as in Fig. 2 except for the absence of a floor and a small change in the lip height and the heat release rate. The flow becomes predominantly vertical everywhere in complete contrast to the fire with a floor. These differences need to be taken into account when using a method belonging to the first three categories discussed above. The predictions show that the velocity increases with height in the region close to the flame, as a result of the increase in temperature with height, while in the region away from the fire, the velocity remains largely unchanged.

NBS-GCR-87-538, California Institute of Technology, 1987.
5. Beyler, C.L. , Ph. D. Thesis, Harvard University. 1983.
6. McCaffrey, B. J. and Cox, G., *National Bureau of Standards,* NBSIR 82- 2473, 1983.
7. Koseki, H. and Yumoto, T., *Fire Technology,* **Feb.**, 33 - 47 (1988).
8. Weckman, E. J., *National Heat Transfer Conference, HTD-Vol. 106, Heat Transfer Phenomea in Radiation, Combustion and Fires,* 399 - 406 (1989).
9. Thomas, P. H., Baldwin, R., and Hesselden, A. J., *Tenth Symposium (International) on Combustion*, 983 - 996 (1983).
10. Zhou, X. C. and Gore, J. P., *Combustion and Flame,* **100**, 52 - 60 (1995).
11. Taylor, G. I. *J. Aerospace Sciences* **25**, 464 (1958).
12. Baum, H. R. and McCaffrey, B. J., *Fire Safety Science Proceedings, 2nd Intl. Symposium,* 129-148 (1989).
13. McCaffrey, B. J., *Combustion and Flame,* **52**, 149 (1983).

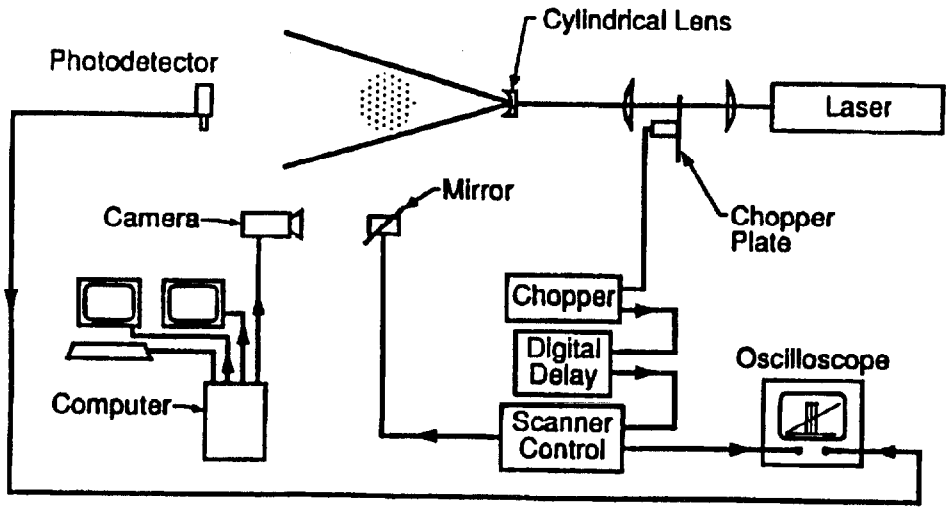

Figure 1. Schematic configuration of the PIV system.

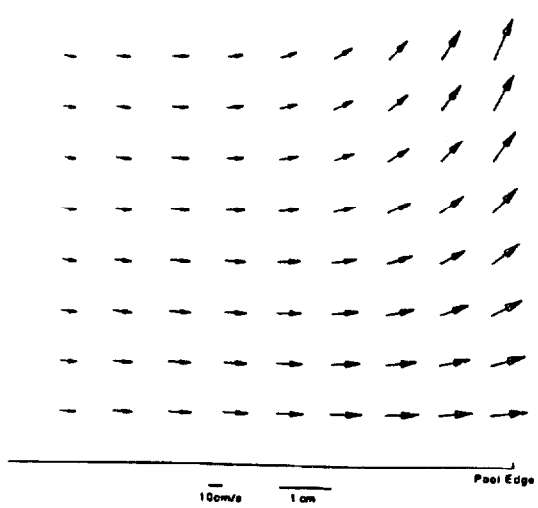

Figure 2. The predicted velocity field induced by a 15 cm pool fire with a floor.

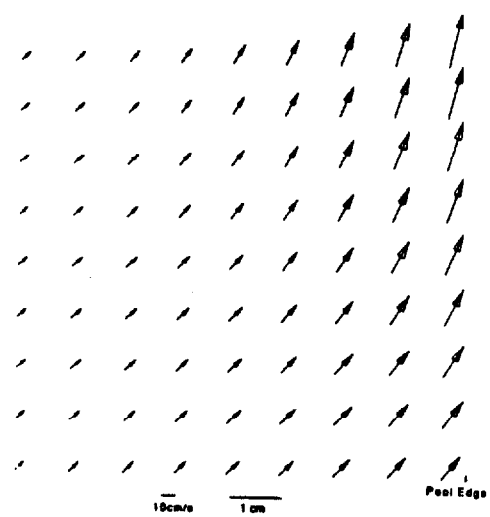

Figure 3. The predicted velocity field induced by a 15 cm pool fire without a floor.

Figure 4 shows the measurements of the mean velocity induced by a 15 cm heptane pool fire with a metal floor, obtained in our laboratory using the PIV system. The predictions in Fig. 2 agree well with the experimentally observed characteristics of the flow field in Fig. 4. The velocity is horizontally inward until the flame boundary is approached, where the vertical velocity component increases. Figure 5 shows the measurements of the mean entrainment flow field for a fire without a floor. The measured radial velocity is much smaller than the axial velocity in this case. These results support the predictions of Fig. 3.

Quantitative comparison of the predicted nondimensional axial velocity U_z^* and the measurements for both cases (with and without floor) at a dimensionless height of $Z^* = 0.1$ as a function of R^* are shown in Fig. 6. The radial distance R, the axial distance Z, the radial velocity U_r and the axial velocity U_Z are nondimensionalized using the same parameters as in Refs. [12] and [13]. For the case with a floor, the predicted axial velocity is almost zero in very good agreement with the measurements. However, the difference between the predictions and the measurements is relatively large for the fire without a floor. Figure 7 shows the comparison between measurements and predictions for the nondimensional radial velocities U_r^*. The discrepancy is larger although the predictions capture the fact that the radial velocity component of the flow induced by a fire with the floor is much larger than that induced by the same fire but without the floor. The discrepancies are most likely a result of the differences in the size and type of the present fires and those used in Ref. [13] in generating the velocity and temperature data used in the specification of $Q(\bar{r})$ and $\omega_\theta(\bar{r})$. McCaffrey [13] also had a floor at some distance below the pool surface. In view of the sensitivity of the velocity field to the presence of a floor, this difference in experimental conditions may be crucial. Indeed, the strongly elliptic nature of the flow makes it extremely difficult to isolate the fire plume from its surroundings.

Conclusions

A kinematic model utilizing existing flame data shows that the flow patterns of the entrainment flow field are dramatically different depending upon whether a floor is present. These differences are in complete agreement with experimental observations. Quantitative predictions of the vertical velocities are satisfactory. However, the radial velocities are overpredicted. Improved correlations for heat release and vorticity distribution in liquid fueled pool fires with appropriate boundary and floor conditions are needed since the data used currently [13] were obtained in 30 cm x 30cm square gas-fired burners and appear to be unsatisfactory for liquid fires.

Acknowledgement

The work at Purdue University is supported by the Center for Fire Research, Building and Fire Research Laboratory, National Institute of Standards and Technology under Grant No. 60NANB2D1291 with Dr. Anthony Hamins and Dr. Takashi Kashiwagi serving as NIST Scientific Officers.

References

1. Ricou, F. P. and Spalding, D. B., *J. Fluid Mech.* **11** : 21-32 (1961).
2. Hill, B. J., *J. Fluid Mech.* **51**: 773-779(1972).
3. Cetegen, B. M., Zukoski, E. E. and Kubota, T., *Combust. Sci. Tech.*, **39**: 305 - 331 (1984).
4. Toner, S. J., Zukoski, E. E. and Kubota, T., *National Bureau of Standards,*

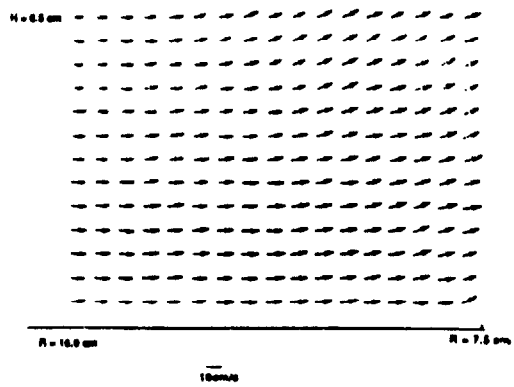

Figure 4. The measured velocity field induced by a 15 cm heptane pool fire with a floor.

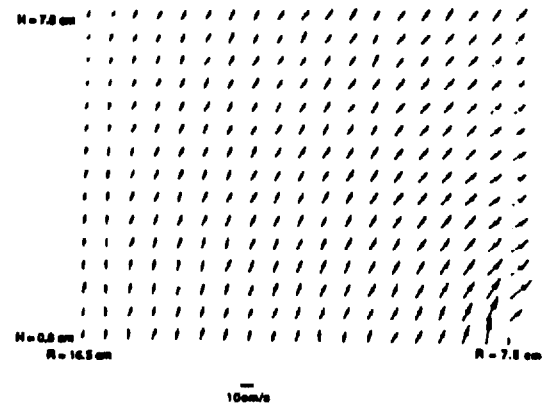

Figure 5. The measured velocity field induced by a 15 cm heptane pool fire without a floor.

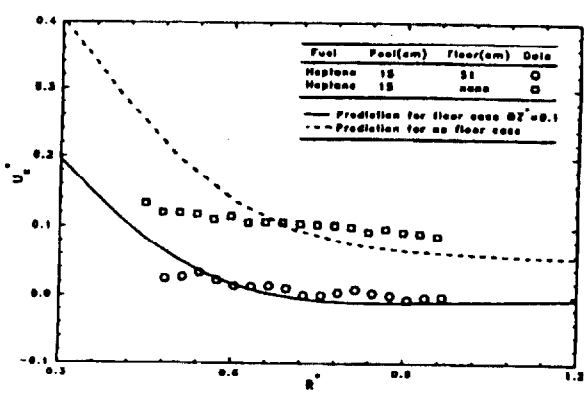

Figure 6. Comparison between predicted and measured nondimensional axial velocity for the fire with and without a floor.

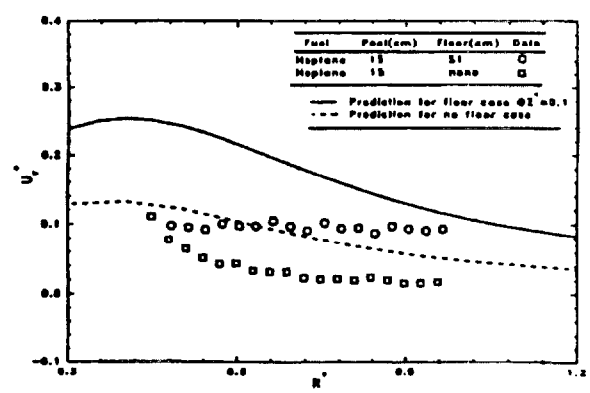

Figure 7. Comparison between predicted and measured nondimensional radial velocity for the fire with and without a floor.

Discussion

Hiroshi Koseki: You made some reference to the data I created. You made some comments about a scale effect. Could you repeat that part again?

Jayavant Gore: Yes. I made it in the context of many other people's work also. In some papers, if they changed R then the intended rate changed and therefore, it's a function of burner size, while some others will say it's not a function of burner size. So I did not want to single out any one. There is room for more work and I know you are doing more work.

Edward Zukoski: It would be very interesting if you could look at what happens near the interface because we use an old Japanese trick of using an incense stick, and the flow is always inward. There was no sign of a big circulation, and you wonder where this air that's coming from the flame goes as it gets to the interface. It did not go out, it always went in towards the fire.

Jayavant Gore: We have not looked at the flow field right here and certainly, we would like to look at it in the future. It becomes very challenging when you go there. It would be very interesting to see what happens to that air. Just the question you pose is very important because if you measure down here, you see a lot of air being set in motion. And if it's traveling up here and it's not going out and it's not going into the plume as indicated in some measurements, where is it going? We'd like to find out. My hypothesis would be that it's going out horizontally this way.